Monthly Notices of the ROYAL ASTRONOMICAL SOCIETY

MNRAS **522,** 1411–1418 (2023) https://doi.org/10.1093/mnras/stad928
Advance Access publication 2023 April 3

The ultraviolet habitable zone of exoplanets

R. Spinelli,[1]★ F. Borsa,[2] G. Ghirlanda,[2,3] G. Ghisellini[2] and F. Haardt[1,2,3]

[1]*Dipartimento di Scienza e Alta Tecnologia, Università dell'Insubria, Via Valleggio 11, I-22100 Como, Italy*
[2]*INAF – Osservatorio Astronomico di Brera, Via E. Bianchi 46, I-23807 Merate (LC), Italy*
[3]*INFN – Sezione Milano–Bicocca, Piazza della Scienza 3, I-20126 Milano, Italy*

Accepted 2023 March 23. Received 2023 February 24; in original form 2022 October 13

ABSTRACT

The dozens of rocky exoplanets discovered in the circumstellar habitable zone (CHZ) currently represent the most suitable places to host life as we know it outside the Solar system. However, the presumed presence of liquid water on the CHZ planets does not guarantee suitable environments for the emergence of life. According to experimental studies, the building blocks of life are most likely produced photochemically in presence of a minimum ultraviolet (UV) flux. On the other hand, high UV flux can be life-threatening, leading to atmospheric erosion and damaging biomolecules essential to life. These arguments raise questions about the actual habitability of CHZ planets around stars other than Solar-type ones, with different UV to bolometric luminosity ratios. By combining the 'principle of mediocrity' and recent experimental studies, we define UV boundary conditions (UV-habitable zone, UHZ) within which life can possibly emerge and evolve. We investigate whether exoplanets discovered in CHZs do indeed experience such conditions. By analysing Swift-UV/Optical Telescope data, we measure the near ultraviolet (NUV) luminosities of 17 stars harbouring 23 planets in their CHZ. We derive an empirical relation between NUV luminosity and stellar effective temperature. We find that 18 of the CHZ exoplanets actually orbit outside the UHZ, i.e. the NUV luminosity of their M-dwarf hosts is decisively too low to trigger abiogenesis – through cyanosulfidic chemistry – on them. Only stars with effective temperature $\gtrsim$3900 K illuminate their CHZ planets with enough NUV radiation to trigger abiogenesis. Alternatively, colder stars would require a high-energy flaring activity.

Key words: Astrobiology – Ultraviolet: stars, planetary systems.

1 INTRODUCTION

In the last 20 yr, exoplanet research has made great strides. More than 5000 exoplanets have been discovered in our Galaxy and more than 8000 candidates are awaiting confirmation from further observations.[1] After an hectic discovery epoch, the research activities are now starting to focus on the characterization of exoplanets with the aim of understanding the planetary population around us and identifying exoplanets with physical properties suitable for life.

Exoplanets around M-dwarf stars may represent the most promising targets to discover habitable worlds. Besides being the most abundant stellar population in our Galaxy (∼75 per cent; Bochanski et al. 2010), M-dwarfs are extremely long-lived and thus offer long time-scales for possible biological evolution within their planetary systems (Shields, Ballard & Johnson 2016). Moreover, the physical properties of M-dwarfs, as their small radii, low masses, and low luminosities favour their habitable zone exoplanets (Kasting, Whitmire & Reynolds 1993; Kopparapu et al. 2013) discovery through methods based on transits and radial velocities (Nutzman & Charbonneau 2008; Quirrenbach et al. 2014). Eventually, M-dwarf habitable zone exoplanets will allow us to perform a characterization of their atmospheres (e.g. Snellen et al. 2013; Rodler & López-Morales 2014; Batalha et al. 2015; Barstow & Irwin 2016; Lustig-Yaeger, Lincowski & Meadows 2019) through spectroscopy by the *JWST* (Gardner et al. 2006) and Extremely Large Telescopes (Gilmozzi & Spyromilio 2007; de Zeeuw, Tamai & Liske 2014).

These studies will possibly include the identification of key biomarkers, such as O_2, O_3, CH_4, and N_2O, whose maintenance on Earth is supported by the presence of life. How to interpret an eventual detection of these biomarkers in the exoplanetary atmospheres is the subject of several works (e.g. Owen 1980; Sagan et al. 1993; Des Marais et al. 2002; Catling et al. 2018; Schwieterman et al. 2018).

On the theoretical side, it is worth investigating whether life can emerge and endure on such worlds. Several factors contribute to the emergence and development of life (at least as we know it) on planets. Given its importance for life on Earth, liquid water is considered a necessary factor. Thus, a rocky planet is considered potentially habitable if it resides in the so-called circumstellar habitable zone (CHZ, e.g. Kasting, Whitmire & Reynolds 1993; Kopparapu et al. 2013), namely the annular region around a star in which there are suitable temperatures for the presence of liquid water on the planet's surface. This region is primarily determined by the star-planet distance and the stellar properties (such as luminosity and effective temperature $T_{\rm eff}$), but it can also depend on other factors such as atmospheric composition (Zsom et al. 2013), planetary mass

★ E-mail: riccardo.spinelli.it@gmail.com
[1]https://exoplanets.nasa.gov/.

(Kopparapu et al. 2014), volcanic activity (Ramirez & Kaltenegger 2017), and tidal locking (Driscoll & Barnes 2015; Barnes 2017).

In addition to the presence of liquid water, other factors may contribute to making a planet habitable (Meadows & Barnes 2018). For example, intrinsic properties of the planet (e.g. ongoing plate tectonics and volcanism) play a crucial role in temperature regulation and may generate magnetic fields that limit atmospheric stripping due to the stellar wind (e.g. Lenardic et al. 2014; Tosi et al. 2017; Godolt et al. 2019; McIntyre 2022).

The radiation environment, determined by the host star and/or other galactic powerful sources, may influence habitability. For example M-dwarfs are known to be strong and variable X-ray/ultraviolet (UV) emitters as a consequence of magnetic activity in their outer atmospheres (France et al. 2012; Stelzer et al. 2013). In particular, the high-energy UV/X-ray emission of the host star may have a crucial role for the habitability of its closest (∼0.1 au) planets. The effect of the high-energy radiation environment on habitability could be twofold. UV/X-ray radiation may cause atmospheric erosion (Sanz-Forcada et al. 2010), biomolecules destruction (Sagan 1973), and damage to various species of proteins and lipids (Buccino, Lemarchand & Mauas 2007). On the larger galactic length-scales (pc to kpc), planetary habitability can also be threatened by powerful astrophysical transient of high-energy radiation, like gamma-ray bursts (GRBs) and supernovae (SNe), which can trigger mass extinction events (Ruderman 1974; Thorsett 1995; Gehrels et al. 2004; Melott & Thomas 2011; Piran & Jimenez 2014; Spinelli et al. 2021). On the other hand, experimental studies (e.g. Toupance, Bossard & Raulin 1977; Powner, Gerland & Sutherland 2009; Ritson & Sutherland 2012; Patel et al. 2015; Rimmer et al. 2018; Xu et al. 2018) demonstrate that UV light is a crucial ingredient for prebiotic photochemistry, namely for the synthesis of ribonucleic acid (RNA), i.e. the building blocks for the emergence of life.

In this work, we study and combine the positive (prebiotic) and negative (atmospheric erosion and biomolecules destruction) roles of stellar UV radiation on potentially habitable exoplanets. We define the ultraviolet habitable zone (UHZ) in Section 2 and compare with a sample of exoplanets, selected in Section 3, for which we evaluate (Section 3) the UV luminosity of the host star by exploiting the existing public observations of the *Ultra-Violet Optical Telescope* (*UVOT*; Roming et al. 2005) onboard the Neil Gehrels *Swift* Observatory (Gehrels et al. 2004). Results are presented in Section 4, where we compare the UV habitable zone with the UV irradiation of selected exoplanets and with their habitable zone as defined by the classical H_2O criterium (Kopparapu et al. 2013). Results are discussed in Section 5.

2 UV HABITABLE ZONE

Assuming that the conditions for the existence of life in the Universe are similar to those on Earth is the 'hard core' (Lakatos 1974) of all programs in search of life in the Universe. Therefore, among all the exoplanets discovered, rocky planets with liquid water on their surface are considered the best candidates for finding life outside the Solar system. For this reason, the search for life forms outside the Solar system focuses on this particular class of exoplanets.

While the presence of liquid water is considered a necessary condition for the maintenance of life, how life actually stems from prebiotic conditions is one of the greatest open questions for the understanding of our very existence. Several studies (see, e.g. Patel et al. 2015; Ranjan, Wordsworth & Sasselov 2017; Xu et al. 2018) suggest scenarios in which the intensity of UV radiation reaching a planet's surface may play a key role in the emergence of life.

This holds only for scenarios that require UV light. Moreover, the specific thresholds depends on the scenario and chemical reactions considered (see Ranjan & Sasselov 2017; Rimmer et al. 2021). The contrasting effects of UV radiation on life, i.e. the action that favours prebiotic activity versus the atmospheric erosion and DNA destruction, define two boundaries that delimit a region around a star where exoplanets are subject to favourable conditions in terms of UV irradiation. We therefore define this region as the *UV–habitable zone*, or UHZ.

Inspired by the so-called 'principle of mediocrity' (von Hoerner 1961), i.e. the idea that the conditions that allowed the origin and evolution of life on Earth are average in comparison with other inhabited worlds in the Universe, Buccino, Lemarchand & Mauas (2007) defined the UHZ as follows. The boundaries of the UHZ are calculated by considering the intensity of UV radiation reaching the Archean Earth (AE) 3.8 Gyr ago, the era of the first traces of life on Earth (Dodd et al. 2017), which we indicate as $S(\mathrm{AE})_{\mathrm{UV}}$. Notice that this symbol refers to the flux incident above the AE atmosphere. With respect to the planet–star separation, Buccino, Lemarchand & Mauas (2007) defines the inner UHZ boundary as the distance corresponding to the maximum tolerable dose of UV radiation for biological systems, i.e. $S_{\mathrm{UV}} < 2\,S(\mathrm{AE})_{\mathrm{UV}}$, and the outer UHZ boundary as the distance corresponding to the minimum flux needed for the chemical synthesis of complex molecules (such as amino acids, lipids, and nucleosides), i.e. $S_{\mathrm{UV}} > 0.5\,S(\mathrm{AE})_{\mathrm{UV}}$. These fluxes are then rescaled accounting for possible absorption by the planet atmosphere to compute the actual flux incident on the planet's surface.

Given their ability to combines with other molecules in aqueous solution and create to important biomolecules for the origin of RNA, hydrogen cyanide (HCN) is considered a fundamental molecules for the origin of life in the context of the RNA world hypothesis (Rich & Kasha 1962; Gilbert 1986). Among these molecules there are amino acid glycine (Miller 1957), nucleobase adenine (Ferris & Orgel L. 1966; Sanchez, Ferris & Orgel 1966; Sanchez & Orgel 1970), lipids, and nucleosides (Ritson & Sutherland 2012; Patel et al. 2015; Xu et al. 2018).

Recently, Rimmer et al. (2018) showed that, by illuminating a mixture of HCN and SO_3^{2-} with near-UV (NUV; 200–280 nm) light, RNA pyrimidine nucleotide precursors are produced. On the contrary, the absence of NUV light in the same mixture leads to the formation of inert adducts with no prebiotic potential. Rimmer et al. (2018) defined the minimum NUV flux required for abiogenesis as the flux which triggers a 50 per cent yield of the photochemical product at temperature of 0°C, in the SO_3^{2-} reaction. This corresponds to integrate a specific flux of 6.8×10^9 photons $\mathrm{cm^{-2}\,s^{-1}\,\AA^{-1}}$ over the 200–280 nm band.

In this work, we consider the experimentally motivated, threshold flux of Rimmer et al. (2018), i.e. $S_{\mathrm{UV}} > 45$ erg $\mathrm{cm^2\ s^{-1}}$, defining the outer boundary of the UHZ. For the maximum tolerable flux, setting the inner UHZ boundary, we consider the criterion of Buccino, Lemarchand & Mauas (2007), i.e. $S_{\mathrm{UV}} < 2 \times S(\mathrm{AE})_{\mathrm{UV}} = 2 \times 5.2 \times 10^3$ erg $\mathrm{cm^{-2}\ s^{-1}}$, where for $S(\mathrm{AE})_{\mathrm{UV}}$ we adopt the solar spectra of Thuillier et al. (2004) and assume that the Sun, during the Archean Eon, was radiating, in the entire 200–280 nm wavelength range, at 75 per cent of its present-day power (Cockell 1998, 2000). Finally, in order to account for atmospheric absorption, we consider that the flux that actually reaches a planet's surface can be 10 per cent, 50 per cent, or 100 per cent of that at the top of the atmosphere (respectively a transmission f of 0.1, 0.5, and

1.0). Here, we do not aim at any frequency-dependent description of atmospheric UV transmission, rather we consider an average value over the relevant frequency range.

3 SAMPLE SELECTION AND DATA ANALYSIS

The aim of the present study is to set the UHZ in the context of exoplanets considered potentially habitable based solely on the classical H_2O criterion, i.e. planets orbiting their host stars in the CHZ. Our targets should satisfy three conditions: (i) be rocky planets, (ii) reside in the CHZ of their host stars for which (iii) NUV observations are available.

3.1 Sample selection

We consider the catalogue of potentially habitable planets provided by the Planetary Habitability Laboratory (PHL, University of Puerto Rico, Arecibo).[2,3] The PHL selects planets with $0.5 \leq R_P \leq 1.6$ or with $0.1 \leq M_P \sin i \leq 3$ and planets with $1.6 \leq R_P \leq 2.5$ or with $3 \leq M_P \sin i \leq 10$ (planetary radii R_P and masses M_P are in Terrestrial units $R_\oplus$ and $M_\oplus$).

The first set of conditions selects Earth-like planets (conservative sample, CS) of probable rocky composition, whereas the second one widens the sample to ocean worlds and mini-Neptunes (optimistic sample, OS). The lower limit of 0.5 $R_\oplus$ (or 0.1 $M_\oplus$) excludes planets not massive enough to retain their atmospheres (Zahnle & Catling 2017).

From the host star luminosity and semimajor axis reported in the PHL, we compute the bolometric insulation received by each planet. Fig. 1 shows all planets of the PHL sample in the stellar $T_{\rm eff}$-insulation plane (CS and OS planets are shown by the grey and blue symbols, respectively).

Next, we need to select those planets which are in the CHZ (see Kopparapu et al. 2013, 2014, for different definitions for the CHZ boundaries). In this work we adopt the optimistic limits of the CHZ, empirically determined by Kasting, Whitmire & Reynolds (1993) and Kopparapu et al. (2013). These limits are based on the inferred presence of liquid water on Mars' surface before 3.8 Gyr ago (Pollack et al. 1987; Bibring et al. 2006), and on the absence of liquid water on Venus' surface for, at least, the past Gyr (Solomon & Head 1991). It is assumed (optimistically) that Venus and Mars actually had liquid water on their surfaces, respectively 1 and 3.8 Gyr ago and therefore that they were habitable at those epochs.

In particular, Kopparapu et al. (2013) estimate the inner edge of the solar CHZ by computing the solar irradiation experienced by Venus 1 Gyr ago when the Sun luminosity was 92 per cent of its present-day value. This flux, computed at Venus–Sun distance, corresponds to 1.76 times the flux received today by the Earth ($S_\oplus = 1.36 \times 10^6$ erg cm^{-2} s^{-1}). The outer edge of the solar CHZ is set by considering the flux received by Mars 3.8 Gyr ago when the solar luminosity was 75 per cent of its present-day value, i.e. $\simeq 0.32\, S_\oplus$. These limiting flux values are defined for Solar-type stars. For stellar types other than solar, Kopparapu et al. (2013) provide corrective factors as function of the stellar $T_{\rm eff}$.

[2]https://phl.upr.edu/the-habitable-exoplanets-catalog.

[3]The PHL catalogue is complete up to 59. Therefore, we updated it to June 2022 by applying the PHL selection criteria to the NASA Exoplanet Archive https://exoplanetarchive.ipac.caltech.edu/. We find 14 more exoplanets with no Swift UVOT observations in the considered filters.

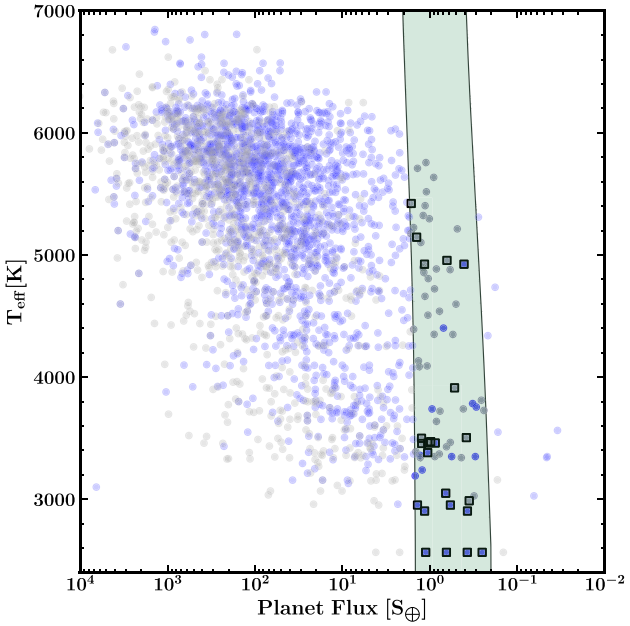

Figure 1. $T_{\rm eff}$ versus planet received flux (in unit of the flux received today by the Earth $S_\oplus = 1.36 \times 10^6$ erg cm^{-2} s^{-1}) above the atmosphere. Grey symbols: discovered planets with $0.5 \leq R_P \leq 1.6$ or with $0.1 \leq M_P \sin(i) \leq 3$ and planets with $1.6 \leq R_P \leq 2.5$ or with $3 \leq M_P \sin(i) \leq 10$ (radii and masses in Terrestrial units). Green zone: the optimistic habitable zone as defined by Kopparapu et al. (2013). Square symbols: planets with archival *Swift*/*UVOT* observations in UM2/UW2/UW1 filters.

Fig. 1 shows the CHZ (green-shaded region) computed according to the definition of Kopparapu et al. (2013). In general, the CHZ is weakly dependent on the stellar $T_{\rm eff}$ and it is bracketed by flux values, received by the planet's atmosphere, 0.2–1.4$S_\oplus$ for low-temperature stars ($T_{\rm eff} < 3000$ K) and 0.4–2$S_\oplus$ for large $T_{\rm eff}$ values.

In order to estimate the host star NUV luminosity, we searched into the *Swift*/*UVOT* archive and found observations for 23 of the 73 selected CHZ targets (grey and blue squares in Fig. 1). This is the final selected sample of planets in the CHZ with UV observations. A list of the corresponding planetary parameters is provided in Table 1.

3.2 *Swift*/*UVOT* data analysis

Swift is a space observatory mainly dedicated to the study of GRB. *Swift* obtains X-ray and UV data simultaneously through the co-aligned X-ray telescope (XRT, 0.2–10 keV – Burrows et al. 2005) and *UVOT* (1700–6500 Å – Roming et al. 2005). For each source in our sample, we collected from the *Swift* archive all the archival *UVOT* observations performed with any of the following filters: UM2 [$\lambda_{\rm eff} = 2231$ Å, full width at half-maximum (FWHM) = 498 Å] and UW2 ($\lambda_{\rm eff} = 2030$ Å, FWHM = 657 Å). *UVOT* images (taken with the UVW2 and UVM2 filters) were analysed with the public `HEASOFT (v6.30)` software package.[4] The most recent version of the calibration data base was used.[5] Photometry was performed within a circular source-extraction region of 5 arcsec in radius centred on the source, with the background extracted from a circular region within a radius of about 20 arcsec, close to the target but free from contamination. For each source, we stacked all the observations

[4]https://heasarc.gsfc.nasa.gov/docs/software/heasoft/.

[5]https://heasarc.gsfc.nasa.gov/docs/heasarc/caldb/.

Table 1. CHZ planets considered in this work, with the spectral type and $T_{\rm eff}$ of the host star, the semimajor axis of the CHZ planet, the flux received by the planet (in the unit of the flux received today by the Earth), the distance from the Earth and the Earth Similarity Index from the PHL.

Star	Spectral Type	$T_{\rm eff}$ [K]	a [au]	S $S_\oplus$	d [pc]	ESI
Trappist−1 d	M8.0	2550	0.022	1.12	12.43	0.91
Trappist−1 e	M8.0	2550	0.029	0.65	12.43	0.85
Trappist−1 f	M8.0	2550	0.038	0.37	12.43	0.68
Trappist−1 g	M8.0	2550	0.047	0.25	12.43	0.58
Teegarden b	M7.0	2790	0.025	1.15	3.83	0.95
Teegarden c	M7.0	2790	0.044	0.37	3.83	0.68
GJ 1061 c	M5.5	2905	0.035	1.45	3.67	0.86
GJ 1061 d	M5.5	2905	0.054	0.69	3.67	0.86
Proxima Cen b	M5.5	3050	0.049	0.65	1.30	0.87
LHS 1140 b	M4.5	3166	0.096	0.50	14.99	0.62
GJ 273 b	M3.5	3382	0.091	1.06	3.79	0.85
GJ 163 c	M3.5	3399	0.125	1.25	15.13	0.69
K2−18 b	M2.5	3464	0.143	1.00	38.03	0.70
GJ 357 d	M2.5	3490	0.204	0.38	9.44	0.58
TOI−700 d	M2.5	3494	0.163	0.85	31.13	0.93
GJ 832 c	M2.0	3601	0.163	0.99	4.96	0.74
GJ 433 d	M2.0	3605	0.178	1.03	9.06	0.74
GJ 229A c	M0.0	3912	0.384	0.53	5.76	0.69
Kepler−62 f	K2.0	4842	0.427	1.35	300.87	0.68
Kepler−62 e	K2.0	4842	0.718	0.48	300.87	0.83
HD 40307 g	K2.0	4867	0.600	0.67	12.94	0.66
Kepler−1606 b	G7.0	5400	0.642	1.29	831.29	0.70
Kepler−1701 b	K1.0	5146	0.561	1.31	584.14	0.71

using the `uvotimsum` tool. We adopted a 3σ detection threshold. Source count rates were then converted into flux densities using the conversion factors given in table 1 of Brown et al. (2016), valid for stellar spectra as given by Pickles (1998).

When available, we analysed and preferably considered data from UM2 filter as it best covers the NUV range. In case no UM2 data were available, we considered UW2 data. In this case, special care was needed as the transmission curve of UW2 is characterized by a red-tail extending in the optical (Breeveld et al. 2011). As a consequence, the integrated flux could be contaminated by the (much brighter) blackbody optical emission from the star's photosphere. In order to correct for such contamination, we adopted the red-tail magnitude corrections as given in table 12 of Brown et al. (2010), which allowed us to disentangle the genuine UV emission from the contaminant stellar blackbody emission. In Table 2, we report the total exposure time, filter, and the average count rate used in this work for each star. For uw2 filter the count rates are already corrected for the red tail contamination.

Table 2. Stars considered in this work with the filter, the total exposure time and the average count rate of the analysed observations. For the uw2 filter the count rates are already corrected for the red tail contamination as described in Section 3.2.

Source	Filter	Exp. time [ks]	Counts s^{-1}
Trappist-1	uw2	274	$(5.32 \pm 1.33) \times 10^{-6}$
Teegarden's star	uw2	34	$(2.75 \pm 0.15) \times 10^{-4}$
GJ 1061	um2	36	0.016 ± 0.002
Proxima Cen	um2	77	1.127 ± 0.038
LHS 1140	uw2	83	0.0314 ± 0.0008
GJ 273	um2	30	0.223 ± 0.002
GJ 163	um2	6	0.065 ± 0.006
K2-18	uw2	12	0.0175 ± 0.0005
GJ 357	uw2	16	0.1416 ± 0.0003
TOI-700	um2	17	0.0096 ± 0.0026
TOI-700	uw2	22	0.015 ± 0.0002
GJ 832	um2	39	0.735 ± 0.016
GJ 433	um2	6	0.297 ± 0.011
GJ 229 A	um2	0.5	2.304 ± 0.090
GJ 229 A	um2	0.6	3.569 ± 0.076
Kepler-62	uw2	5	0.0266 ± 0.0018
HD 40307	um2	1.5	16.645 ± 0.368
Kepler-1606	um2	0.7	0.046 ± 0.012
Kepler-1701	um2	1.7	0.036 ± 0.009

4 RESULTS

The NUV luminosity $L_{\rm NUV}$ for all the stars in our sample were estimated through the stellar distances of GAIA DR2 (Gaia Collaboration 2018). To this aim we assumed a flat-spectrum (in erg cm^{-2} s^{-1} $Å^{-1}$) in the NUV band, as supported by visual inspection of archival NUV data obtained by *Hubble Space Telescope*/Space Telescope Imaging Spectrograph and spectra delivered by the treasury MUSCLES survey (France et al. 2016).

Fig. 2 shows the NUV luminosity $L_{\rm NUV}$ versus the star–planet separation a. In this plane the UHZ is represented as a stripe, bounded by the inner and outer values defined in Section 2. We considered three different NUV atmospheric transmission values: 10 per cent (violet), 50 per cent (red), and 100 per cent (grey). Our targets are shown (circles) in the $L_{\rm NUV} - a$ according to the NUV luminosity we derived from *Swift–UVOT* data analysis. The horizontal line on each planetary system shows the extension of the relative CHZ. The latter is derived as in Kopparapu et al. (2013) from the star's bolometric luminosity and $T_{\rm eff}$. Fig. 2 allows us to compare the CHZ of specific stellar systems to the UHZ.

It is interesting to relate $L_{\rm NUV}$ (erg s^{-1}) to the stellar $T_{\rm eff}$ (K), and estimate the CHZ from there. To this aim, we fit a log–log relation

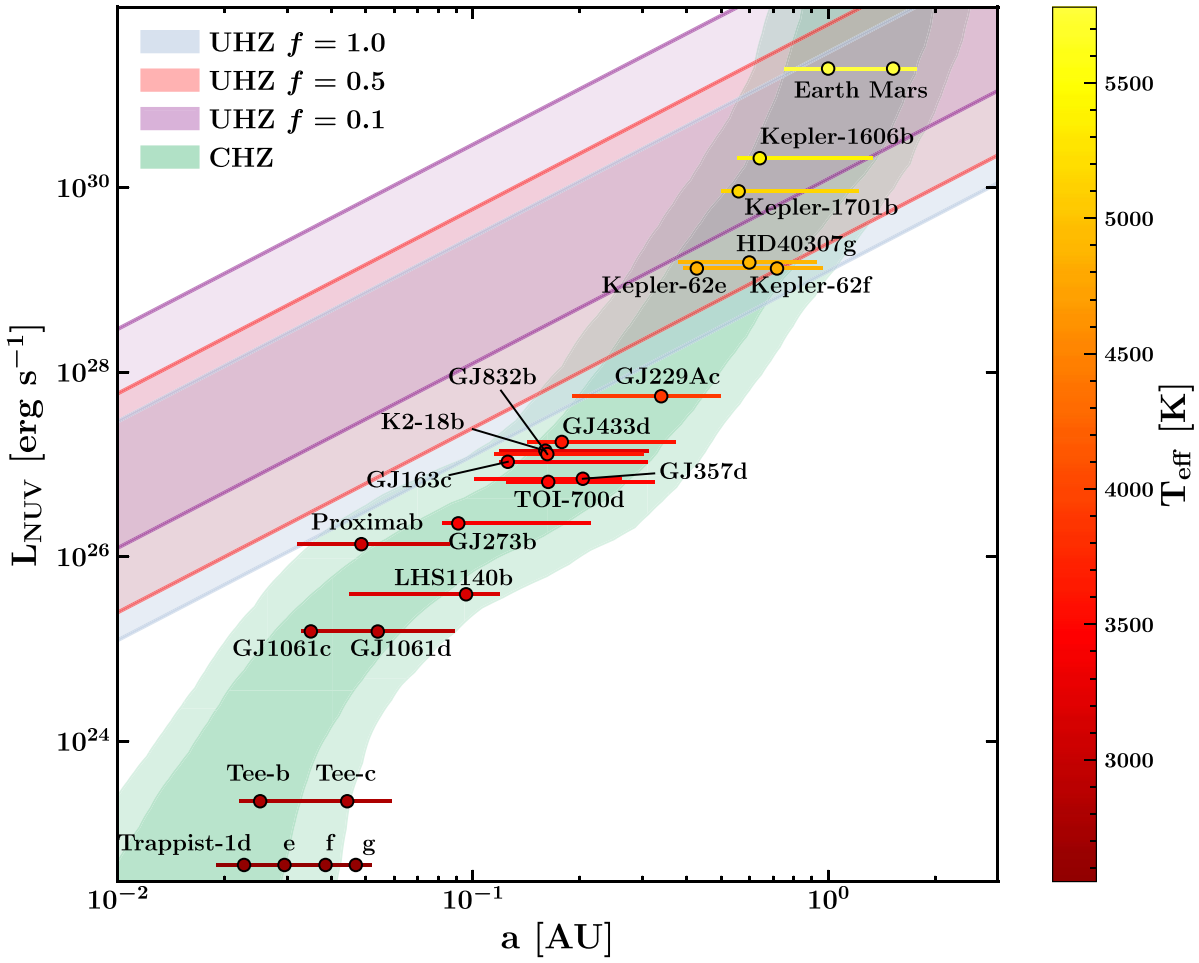

Figure 2. NUV (near ultraviolet) luminosity versus star–planet separation. The UHZ (ultraviolet habitable zone, see Section 2) is defined by the inner (outer) boundary corresponding to the maximum (minimum) UV flux tolerable required) for life resilience (abiogenesis, considering a specific prebiotic pathways). Three UHZ are shown corresponding to 100 per cent, 50 per cent, and 10 per cent (as labelled) atmospheric transmission (f), to the planet's surface, of the UV flux at the top of the atmosphere. The planets of our sample (Section 3) selected for being in the CHZ (Circumstellar Habitable Zone) and having UV observations (thus providing L_{NUV}) are shown by the circle symbols. The colour coding corresponds to the T_{eff} of their host stars (vertical colour bar). The horizontal bar of each exoplanet shows the CHZ as derived by Kopparapu et al. (2013). The green-shaded regions show the CHZ as derived through the $L_{NUV} - T_{eff}$ correlation (Section 5).

between our measured L_{NUV} and T_{eff}, where the latter was obtained from the TESS Input Catalogue (TIC, Stassun et al. 2019) for most of our targets. For Proxima Centauri, GJ 273, GJ 832, Trappist-1, and GJ 229A no T_{eff} was reported in the TIC and the values are respectively from Anglada-Escudé et al. (2016), Astudillo-Defru et al. (2017), Turnbull (2015), Gillon et al. (2017), and Gaia Collaboration (2018). The $T_{eff} - L_{NUV}$ data are shown in Fig. 3. A simple least-squares fit produces the following log–log relation:

$$\log_{10} L_{NUV} = (21.12) \log_{10} T_{eff} - (48.22). \quad (1)$$

The relation between T_{eff} and NUV luminosity (equation 1 above) is a steep power-law ($L_{NUV} \propto T_{eff}^{21}$). This can be justified considering that for a blackbody spectrum, the ratio F_{NUV}/F_{bol} is approximately $\propto T_{eff}^{12}$ (i.e. the colder is the star the more the NUV band samples the blackbody Wien tail). Moreover, in the range $2800 \lesssim T_{eff} \lesssim 6000$ K, the stellar radius $R_\star$ is approximately $\propto T_{eff}^{2.5}$. As a result, from the Stefan–Boltzmann law ($F_{bol} \propto T_{eff}^4$) we obtain $L_{NUV} \propto F_{NUV} R_\star^2 \propto T_{eff}^{21}$. In Fig. 2 stars are colour-coded according to their T_{eff} (red to yellow colours going from M-type to G-type stars).

Adopting the relations from the Baraffe stellar evolutionary models (Baraffe et al. 1998), we obtained a stellar radius-T_{eff} relation through which we estimated the bolometric luminosity L_{bol} from the Stefan–Boltzmann law. With T_{eff} an L_{bol} at hand, we could rely on the very definition of CHZ given by Kopparapu et al. (2014), who indeed defined the CHZ in terms of the bolometric flux received as a function of the stellar T_{eff}. With equation (1), we estimated the orbital boundaries of the CHZ as a function of T_{eff}: this is shown by the curved shaded region in Fig. 2. The dark (light) green regions in Fig. 3 were obtained by shifting the relation given by equation (1) by 1σ (3σ).

Fig. 2 shows that the agreement between the CHZ measured from the NUV luminosity (horizontal bars on each symbol) and that based on bolometric luminosity and T_{eff} (curved green stripes) is generally good, though some notably exceptions stand out. For instance, Proxima has a reported T_{eff} such that it lies above the fitted

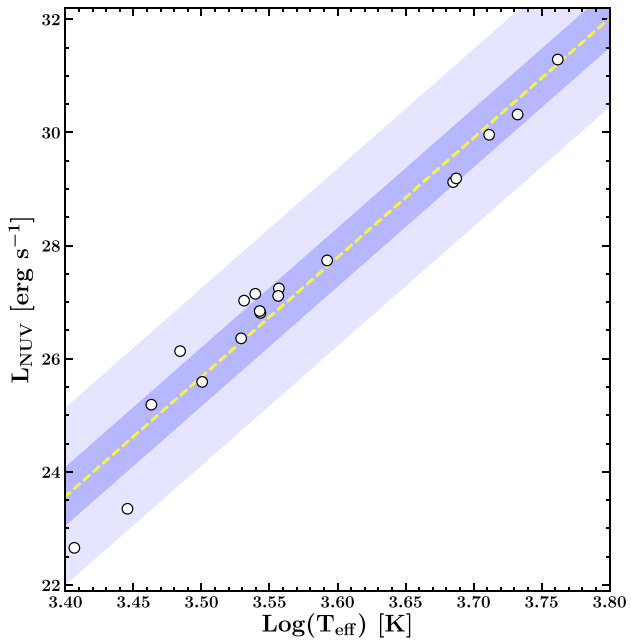

Figure 3. Correlation between L_{NUV} and T_{eff}. Open symbols represent our target sample for which we estimated L_{NUV} from the available *Swift*/*UVOT* observations. The yellow dashed line is a least-squares fit of the data points. The shaded regions show the 1σ and 3σ dispersion of the data point around the best-fitting line. The dispersion is measured as the σ parameter of the Gaussian distribution of the distances (computed perpendicular) of the data points from the best-fitting line. Proxima Centauri is the fourth source from the left.

L_{NUV}–T_{eff} relation of Fig. 3, hence the two different estimates of Proxima's CHZ appear somewhat off in Fig. 2.

5 DISCUSSION

In Fig. 2, the UV luminosity L_{NUV} of the host star is plotted against the planet-to-star distance a. Rocky planets located in the CHZ of their host stars with available UV observations are shown as open circles. For each planet, the CHZ is represented by the horizontal bar which delimits the specific range of a where H_2O can be present in liquid phase on planet's surfaces. The shaded (blue, red, and violet) diagonal stripe in Fig. 2 represents the combination of L_{NUV} and a where abiogenesis can actually occur and the UV irradiation is sustainable by planets' biota.

The main conclusion that can be drawn from Fig. 2 is that the averaged NUV luminosity of M-dwarfs is too low to trigger abiogenesis, through the considered pathways, on planets located within their respective CHZ (see also Ranjan & Sasselov 2017; Rimmer et al. 2018). Even in the extreme case of atmospheres completely transparent to NUV radiation ($f = 1.0$, grey diagonal stripe), CHZ bars do not intersect the UHZ stripe, except in the case of Proxima Centauri. Indeed, the very inner edge of the habitable zone of Proxima Centauri, which has a particularly high NUV emission given its T_{eff}, overlaps with the UHZ zone ($f = 1.0$, grey diagonal stripe), though the actual position of the Proxima Centauri b lies out of this region. We must note that planets around M-dwarfs may still be subject to abiogenesis, provided their host stars are characterized by intense and frequent NUV flare activity (Günther et al. 2019; Murray et al. 2022) or during the early stages of stellar evolution (Chavali et al. 2022).

Our analysis of *UVOT* observations allowed us to derive an empirical relation between the L_{NUV} and T_{eff} (equation 1 and Fig. 3). Furthermore, through stellar models (Baraffe et al. 1998) providing radii and bolometric luminosities, we can infer the CHZ as defined in Kopparapu et al. (2014) (shaded green curved region in Fig. 2). The intersection between the UHZ and the CHZ is limited by a threshold temperature which excludes most M-dwarfs. According to the transparency of the atmosphere (here parametrized with f which represents the fraction of transmitted flux), we find that for the completely transparent case ($f = 1.0$) stars with $T_{eff} \gtrsim 3900$ K may have experienced the correct NUV flux (sufficient for abiogenesis and not too high to be dangerous for biota). Such threshold temperature increases to $T_{eff} \gtrsim 4200$ K if $f = 0.5$ (red-shaded region) and $T_{eff} \gtrsim 4700$ K if $f = 0.1$ (violet-shaded region).

It is worth noting here that we neglected any transformation of the atmosphere induced by the absorbed UV radiation. As an example, let's consider an atmosphere fully opaque to UV radiation, i.e. the planetary surface is shielded from energetic photons. This can be positive for present-life, but negative for the possibility of UV-triggered abiogenesis. At the same time the atmosphere could be transformed over time by the absorbed UV radiation, possibly driving an evolution of the transmission properties over time, and then an evolution of the UHZ for a specific planet. A detailed discussion of these issues is beyond the scope of this work.

We must also note that we used the L_{NUV}–T_{eff} relation reported in equation (1) only for the purpose of representing the H_2O habitable zone in Fig. 2. Indeed, the steepness of the correlation prevents its use to estimate the NUV luminosity given T_{eff}, a small difference in temperature can lead to orders of magnitudes differences in L_{NUV}. This owns a particular relevance in view of the different estimates of T_{eff} often present in the literature (up to hundreds degrees) for the very same star (see, e.g. the NASA Exoplanet Archive[6]). It is therefore clear that direct NUV data are necessary.

In our derivation of the UHZ shown in Fig. 2, we considered the flux threshold needed to trigger abiogenesis proposed by Rimmer et al. (2018). This is the flux leading to a 50 per cent yield of the photochemical products at 0°C in the SO_3^{2-} reaction (Section 2). As discussed by Rimmer et al. (2018) this choice is very liberal, since any prebiotic synthesis will take several steps, and even a 50 per cent yield per step will probably result in too small a final concentration of life's building blocks to do anything (see the discussion of the 'arithmetic demon' in Rimmer et al. 2018). Relaxing the per cent yield will only work if prebiotic chemists find a way to stepwise concentrate preferentially low yield products.

In this case, if we allow for lower yields, i.e. for a lower flux value, the abiogenesis limit will consequently shift to the right in Fig. 2. As an example, at 0°C, the flux required to obtain a 25 per cent and a 10 per cent yield is a factor of 4 and 20 less than that required to obtain a 50 per cent yield (see fig. 3 in Rimmer et al. 2018). On the contrary, if we assume a larger temperature, the abiogenesis limit would shift to the left, since a higher flux is required for the same yield at higher temperatures (see fig. 3 in Rimmer et al. 2018). As an example, at 20°C and at 40°C the NUV flux required is ∼25 and ∼250 times higher than that required at 0°C to have a 50 per cent yield. The right boundary of the UHZ would scale linearly with these factors.

In order to estimate the inner boundary of UHZ (Section 2), inspired by the Principle of Mediocrity we assumed the maximum tolerable NUV flux as twice the flux experienced by the AE above

[6]https://exoplanetarchive.ipac.caltech.edu/.

the atmosphere. If life can resist a larger NUV flux, then a planet can orbit closer to its star. This corresponds to shifting the limits of the UHZ zone in Fig. 2 to the left.

In our work, we did not consider possible effects caused by the Far-UV radiation (FUV; <200 nm). While FUV radiation is important in the context of atmospheric photochemistry, it is most probably unable to reach the surface of habitable planets because of severe absorption by atmospheric constituents, such as water vapor and carbon dioxide (Cnossen et al. 2007; Ranjan & Sasselov 2017).

In is important to realize that the prebiotic pathways we considered are not the only possible for explaining the origin of life (e.g. Cleaves et al. 2008; Rui-Mirazo, Briones & de la Escosura 2013). What is particularly intriguing is that the UV-criterion for abiogenesis was derived through laboratory experiments, that showed how much UV radiation is required to form RNA pyrimidines (Powner et al. 2009; Ritson & Sutherland 2012; Patel et al. 2015; Rimmer et al. 2018; Xu et al. 2018). This finding is supported also by the fact that RNA exhibits selection pressure under UV radiation, suggesting that it is formed in a UV-rich environment (Rios A. & Tor 2013; Beckstead et al. 2016; Pollum et al. 2016). Moreover, as shown by Deamer & Weber (2010), UV radiation was by far the most abundant source of chemical free energy present on the surface of the early Earth.

As suggested by Lillo-Box et al. (2022), K-type stars may currently be the best candidates for searching planets with suitable conditions for life as we know it. Due to their closer CHZ, the CHZ planet detection via transit and/or radial velocity is easier compared to G-stars. Moreover, K-type stars are longer-lived with respect to G-star and thus they offer longer time-scales for biological evolution on their orbiting planets. In contrast with M-dwarfs, the lower activity/variability of K-stars favours detectability and habitability. Furthermore, compared to M-dwarfs, the habitable planets around K-stars are not tidal-locked (Heller, Leconte & Barnes 2011; Barnes 2017). In our study, we further demonstrated that K-stars can irradiate planets in the CHZ with a NUV flux sufficient to trigger abiogenesis.

In the next decades exoplanetary research will be able to carry out statistical studies on the presence of biosignatures in the atmosphere of exoplanets. This brings about a change of perspective, turning exoplanets into laboratories for testing theories about the origin of life. Should we find life on a planet around M-dwarfs, we will have to imagine another mechanisms able to provide the necessary UV flux in these stars (e.g. flares or early stages of stellar evolution), or we will have to reject the prebiotic pathways to life we considered here.

ACKNOWLEDGEMENTS

This study made use of data supplied by the UK *Swift* Science Data Centre at the University of Leicester. Part of this work is based on archival data, software, or online services provided by the Space Science Data Center-ASI. RS acknowledges Sergio Campana and Claudia Scarlata for the suggestions regarding the *Swift–UVOT* data analysis and Jacopo Pravettoni for the valuable support for data visualization. We also thank the referee, Paul Rimmer, for the helpful comments and suggestions that improved the quality of the paper.

DATA AVAILABILITY

The data underlying this article are available in the Swift Data Archive Mirror, see: https://www.ssdc.asi.it/mmia/index.php?mission=swiftmastr.

REFERENCES

Anglada-Escudé G. et al., 2016, Nature, 536, 437
Astudillo-Defru N. et al., 2017, A&A, 602, A88
Baraffe I., Chabrier G., Allard F., Hauschildt P. H. 1998, A&A, 337, 403
Barnes R., 2017, Celest. Mech. Dyn. Astron., 129, 509
Barstow J. K., Irwin P. G. J., 2016, MNRAS, 461, L92
Batalha N., Kalirai J., Lunine J., Clampin M., Lindler D., 2015, preprint (arXiv:1507.02655)
Beckstead A. A., Zhang Y., de Vries M. S., Kohler B., 2016, Phys. Chem. Chem. Phys., 18, 24228
Bibring J.-P. et al., 2006, Science, 312, 400
Bochanski J. J. et al., 2010, AJ, 139, 2679
Breeveld A. A., Landsman W., Holland S. T., Roming P., Kuin N. P. M., Page M. J., 2011, in McEnery J. E., Racusin J. L., Gehrels N., eds, AIP Conf. Proc. Vol. 1358, Gamma Ray Bursts 2010. Am. Inst. Phys., New York, p. 373
Brown P. J. et al., 2010, ApJ, 721, 1608
Brown P. J. et al., 2016, VizieR Online Data Catalog, J/AJ/152/102
Buccino A. P., Lemarchand G. A., Mauas P. J. D., 2007, Icarus, 192, 582
Burrows D. N. et al., 2005, Space Sci. Rev., 120, 165
Catling D. C. et al., 2018, Astrobiology, 18, 709
Chavali S., Youngblood A., Paudel R. R., Loyd R. O. P., Molaverdikhani K., Pineda J. S., Barclay T., Vega L. D., 2022, Res. Note. Am. Astron. Soc., 6, 201
Cleaves H. J., Chalmers J. H., Lazcano A., Miller S. L., Bada J. L., 2008, Orig. Life Evol. Biosph., 38, 105
Cnossen I., Sanz-Forcada J., Favata F., Witasse O., Zegers T., Arnold N. F., 2007, J. Geophys. Res. (Planets), 112, E02008
Cockell C. S., 1998, J. Theor. Biol., 193, 717
Cockell C. S., 2000, Planet. Space Sci., 48, 203
Deamer D, Weber A. L., 2010, Cold Spring Harb. Perspect. Biol., 2, a004929
Des Marais D. J. et al., 2002, Astrobiology, 2, 153
Dodd M. S., Papineau D., Grenne T., Slack J. F., Rittner M., Pirajno F., O'Neil J., Little C. T. S., 2017, Nature, 543, 60
Driscoll P. E., Barnes R., 2015, Astrobiology, 15, 739
de Zeeuw T., Tamai R., Liske J., 2014, The Messenger, 158, 3
Ferris J. P., Orgel L. E., 1966, J. Am. Chem. Soc., 88, 1074
France K., Linsky J. L., Tian F., Froning C. S., Roberge A., 2012, ApJ, 750, L32
France K. et al., 2016, ApJ, 820, 89
Gaia Collaboration, 2018, A&A, 616, A1
Gardner J. P. et al., 2006, Space Sci. Rev., 123, 485
Gehrels N. et al., 2004, ApJ, 611, 1005
Gilbert W., 1986, Nature, 319, 618
Gillon M. et al., 2017, Nature, 542, 456
Godolt M., Tosi N., Stracke B., Grenfell J. L., Ruedas T., Spohn T., Rauer H., 2019, A&A, 625, A12
Günther M. N. et al., 2019, Nature Astron., 3, 1099
Heller R., Leconte J., Barnes R., 2011, A&A, 528, A27
Kasting J. F., Whitmire D. P., Reynolds R. T., 1993, Icarus, 101, 108
Kopparapu R. K. et al., 2013, ApJ, 765, 131
Kopparapu R. K., Ramirez R. M., SchottelKotte J., Kasting J. F., Domagal-Goldman S., Eymet, V., 2014, ApJ, 787, L29
Lakatos I., 1974, in Lakatos I., Musgrave A., eds, Criticism and the Growth of Knowledge, Falsification and the Methodology of Scientific Research Programs. Cambridge Univ. Press, Cambridge, p. 91
Lenardic A. et al., 2014, AGU Fall Meeting Abstracts
Lillo-Box J. et al., 2022, A&A, 667, A102
Lustig-Yaeger J., Lincowski A., Meadows V., 2019, Am. Astron. Soc., 158, 27
McIntyre S. R. N., 2022, A&A, 662, A15
Meadows V. S., Barnes R. K., 2018, in Deeg H. J., Belmonte J. A., eds, Handbook of Exoplanets. Springer International Publishing, Cham, p. 57
Melott A. L., Thomas B. C., 2011, Astrobiology, 11, 343
Miller S. L., 1957, Biochim. Biophys. Acta, 23, 480

Murray C. A. et al., 2022, MNRAS, 513, 2615
Nutzman P., Charbonneau D., 2008, PASP, 120, 317
Owen T., 1980, Strategies for the Search for Life in the Universe, 83, 177
Patel B. H., Percivalle C., Ritson D. J., Duffy C. D., Sutherland J. D., 2015, Nature Chem., 7, 301
Pickles A. J., 1998, PASP, 110, 863
Piran T., Jimenez R., 2014, Phys. Rev. Lett., 113, 231102
Pollack J. B., Kasting J. F., Richardson S. M. Poliakoff K. 1987, Icarus, 71, 203
Pollum M., Ashwood B., Jockusch S., Lam M., Crespo-Hernández C. E., 2016, J. Am. Chem. Soc., 138, 11457
Powner M. W., Gerland B., Sutherland J. D., 2009, Nature, 459, 239
Quirrenbach A. et al., 2014, Proc. IAU Symp. 299, Exploring the Formation and Evolution of Planetary Systems. Kluwer, Dordrecht, p. 395
Ramirez R. M., Kaltenegger L., 2017, ApJ, 837, L4
Ranjan S., Sasselov D. D., 2017, Astrobiology, 17, 169
Ranjan S., Wordsworth R., Sasselov D. D., 2017, ApJ, 843, 110
Rich A., Kasha M., 1962, in Kasha M., Pullman B., eds, Horizons in Biochemistry. Academic Press, New York, p. 103
Rimmer P. B., Xu J., Thompson S. J., Gillen E., Sutherland J. D., Queloz D., 2018, The Origin of RNA Precursors on Exoplanets. American Association for the Advancement of Science
Rimmer P. B., Thompson S. J., Xu J., Russell D. A., Green N. J., Ritson D. J., Sutherland J. D., Queloz D. P. 2021, Astrobiol., 21, 1099
Rios A. C., Tor Y., 2013, Israel J. Chem., 53, 469
Ritson D., Sutherland J. D., 2012, Nature Chem., 4, 895
Rodler F., López-Morales M., 2014, ApJ, 781, 54
Roming P. W. A. et al., 2005, Space Sci. Rev., 120, 95
Ruderman M. A., 1974, Science, 184, 1079
Rui-Mirazo K., Briones C., de la Escosura A., 2013, Chem. Rev. 2014, 114, 285
Sagan C., 1973, J. Theor. Biol., 39, 195
Sagan C., Thompson W. R., Carlson R., Gurnett D., Hord C., 1993, Nature, 365, 715
Sanchez R. A., Orgel L. E., 1970, J. Mol. Biol., 47, 531
Sanchez R. A., Ferris J. P., Orgel L. E., 1966, Science, 154, 784
Sanz-Forcada J., Ribas I., Micela G., Pollock A. M. T., García-Álvarez D., Solano E., Eiroa C., 2010, A&A, 511, L8
Schwieterman E. W. et al., 2018, Astrobiol., 18, 663
Shields A. L., Ballard S., Johnson J. A., 2016, Phys. Rep., 663, 1
Snellen I. A. G., de Kok R. J., le Poole R., Brogi M., Birkby J., 2013, ApJ, 764, 182
Solomon S. C., Head J. W., 1991, Science, 252, 252
Spinelli R., Ghirlanda G., Haardt F., Ghisellini G., Scuderi G., 2021, A&A, 647, A41
Stassun K. G. et al., 2019, AJ, 158, 138
Stelzer B., Marino A., Micela G., López-Santiago J., Liefke C., 2013, MNRAS, 431, 2063
Thorsett S. E., 1995, ApJ, 444, L53
Thuillier G., Floyd L., Woods T. N., Cebula R., Hilsenrath E., Hersé M., Labs D., 2004, Adv. Space Res., 34, 256
Tosi N. et al., 2017, A&A, 605, A71
Toupance G., Bossard A., Raulin F., 1977, Orig. Life, 8, 259
Turnbull M. C., 2015, preprint (arXiv:1510.01731)
von Hoerner S., 1961, Science, 134, 1839
Xu J., Ritson D. J., Ranjan S., Todd Z. R., Sasselov D. D., Sutherland J. D., 2018, Chem. Commun., 54, 5566
Zahnle K. J., Catling D. C., 2017, ApJ, 843, 122
Zsom A., Seager S., de Wit J., Stamenković, V., 2013, ApJ, 778, 109

This paper has been typeset from a TEX/LATEX file prepared by the author.